

**Mechanisms of *Escherichia coli* Inactivation during Solar Driven Photothermal
Disinfection**

Supplementary information

Yibo Hong^a, Weiye Shi^{a,b}, Hao Wang^a, Defang Ma^{a,*}, Yiran Ren^a, Yan Wang^a, Qian
Li^a, Baoyu Gao^a

^a Shandong Key Laboratory of Water Pollution Control and Resource Reuse, School
of Environmental Science and Engineering, Shandong University, Qingdao 266200,
China

^b No.1 Institute of Geology and Mineral Resources of Shandong Province, Ji'nan
250014, China

* Corresponding Author: Defang Ma, E mail: defangma@sdu.edu.cn

Preparation of CNT photothermal film

CNT-COOH powder and dodecylbenzene sulfonic acid in a mass ratio of 1:10 were dissolved in Milli-Q water and ultrasonicated for 1 h to prepare an aqueous mixture with the CNT concentration of 0.1 wt%. Then a 3:1 PVA-CNT solution was sonicated and deposited onto a PVDF membrane under pressure. After that, the prepared membrane was fixed in a crosslinked solution which contains 1 g/L of glutaraldehyde at a pH of 2 for 2 h. Finally, the membrane was dried at 80 °C for 5 min and cooled to room temperature, after which a CNT photothermal film modified membrane was prepared successfully. Before application in solar driven photothermal disinfection, the CNT modified membrane was rinsed several times with Milli-Q water to remove any possible chemical residues.

Solar driven photothermal reactor

The solar driven photothermal reactor with a working volume of 30 mL (30 mm×50 mm×20 mm) consisted of the upper and lower parts to assure the CNT film could be tightly clamped in the reactor without leaking water. The reactor was made of polycarbonate that is heat-resistance. A quartz glass window (30 mm×60 mm×3 mm) was set into the top plate to maximize the solar radiation onto the photothermal film. A xenon lamp solar simulator (Aulight Beijing, CEL HXF300) equipped with AM 1.5 G optical filter was used to provide the solar radiation. Wavelength of simulated solar spectrum was measured by fiber optical spectrometer (Aulight Beijing, AULTT-P4000) and shown in Figure S2.

Characterization of CNT photothermal film

The morphology of the CNT photothermal film was characterized by scanning electron microscopy (SEM, FEI, Quanta 250 FEG). The hydrophilicity was analyzed by contact angle with a contact goniometer (Harker) using deionized water. Atomic force microscope (AFM, Nano Wizard 4) was used to characterize the surface roughness of the CNT film. The bacteriostatic properties of the film were determined by the bacteriostatic circle: putting the film on a culture dish which was evenly coated with bacterial liquid and incubated overnight in 37 °C. The photothermal conversion performance of the film was characterized by measuring the temperatures of the film surface and the water under simulated solar radiation. The photothermal film was inserted into the custom reactor and the surface temperature of the film was measured under direct irradiation of 1 sun using an infrared thermometer (testo 830-T4, equipped with external thermocouple). The temperature of the bulk water (5 mL and water depth 4 mm) injected into the reactor was measured by a K type thermocouple (testo). Thermal images of the film with 0.21 mg/cm² CNT were taken by infrared thermal imager (Hti, HT-201).

Bacteria cultures

Escherichia coli ATCC25922 was selected as the model bacterium. To acquire a stock, cells were transferred to a trypticase soy agar plate and incubated for 24 h at 37 °C. The obtained strains were stored at -4 °C in dark and transferred every two weeks to maintain bacterial activity. An inoculated ring strain *E. coli* was taken from the plate and transferred to tryptic soy broth and then incubated in a shaking incubator overnight. The pellet cell was harvested by centrifugation at 4000 ×g for 3 min and washed twice with phosphate-buffered saline (PBS) to remove cultures. It was resuspended in PBS and diluted to obtain initial cell concentrations of ~10⁵ CFU/mL and ~10⁸ CFU/mL,

turbidity (measured by turbidity instrument, HACH, 2100Q) were 0.42 NTU and 565 NTU, respectively.

Disinfection control experiments

The experiments were separated into 2 parts with solar radiation control and thermal control. In static disinfection experiments, 5 mL diluted cell suspension ($\sim 10^5$ CFU/mL) was added into the reactor. In continuous-flow disinfection, *E. coli* cell suspension ($\sim 10^5$ CFU/mL) stored in an airtight sterile container under constant stirring was injected into the photothermal disinfection reactor at different HRT by a peristaltic pump. Effluent samples were taken for measurement of bactericidal efficiency at certain intervals until the effluent bacterial level became stable. Solar radiation control experiments were tested in the same reactor under 1 sun solar radiation without the photothermal film. For thermal control experiments, a certain volume of stock *E. coli* suspension was spiked into 5 mL sterilized PBS solution that had been heated to 57.1 °C to an *E. coli* concentration of $\sim 10^5$ CFU/mL. Immediately, the 57.1 °C *E. coli* working solution was injected into the reactor which had been preheated to 57.1 °C, the average water temperature in the photothermal system after 20 min of radiation. After disinfection experiments, the treated samples were immediately transferred to the -4 °C refrigerator.

Determination of ROS

Intracellular ROS generation was assessed by the enhancement of fluorescence intensity. H_2DCFDA and DHE were separately dissolved into dimethyl sulfoxide (DMSO) to prepare stock solutions (10mM), which were stored at -20 °C. Before staining, stock solutions were diluted to 10 μM with PBS. The work solution was added to cell suspension with concentration of about 10^8 CFU/mL in a volume ratio of 1:1 and incubated in 37 °C for 60 min. Then, the fluorescently-labeled cell suspension was treated with different disinfection methods for 20min. Treated cells were collected by centrifugation at $6000 \times g$ for 3 times. Fluorescent signals were quantified by microplate spectrophotometer (Tecan Spark, American) at the extinction/ emission wavelengths of 488/529 nm and 518/610 nm for H_2DCFDA and DHE stained cells, respectively.

Cell fixation specimen preparation for SEM

Treated cells collected by centrifugation were fixed at 4 °C through immersing in 2.5% glutaraldehyde (prepared in 1×PBS) for 3 h, then washed the supernatant for 3 times with PBS. After fixation, cells were dehydrated in 30%, 50%, 70%, 80% and 90% ethanol solution for 15 min successively, followed by dehydration in 100% ethanol solution twice. Dispersing the bacterial suspension, then placing a drop of suspension onto the cover glass and drying in a critical point dryer. Before imaging, samples were sputter-coated with Pt.

The viable but non-culturable state (VBNC) of bacteria after photothermal disinfection

To determine whether the bacteria in viable but non-culturable state (VBNC) was existed after photothermal disinfection, the *E. coli* samples were stained after 20 min of photothermal disinfection by PI and Syto 63, and analyzed by flow cytometry. The amount in quadrant IV (PI negative and Syto positive) was only 0.16% (Figure S13). It indicates that photothermal disinfection results in little VBNC bacteria and ensures great water safety.

Photothermal disinfection of Gram-positive bacteria

Staphylococcus aureus was selected as the representative of the gram-positive bacteria, and all experimental procedures were the same as *E. coli* inactivation. From Figure S14A, photothermal treatment inactivated 5-log gram-positive bacteria in 10 min, much faster than gram-negative bacteria (*E. coli*) inactivation. Combining sunlight and heat can also completely kill *Staphylococcus aureus*, but it takes a slightly longer time of 16 min. According to intracellular ROS detection in Figure S14B, *Staphylococcus aureus* rapidly accumulated ROS under photothermal stimulation and reaches its highest point at 10 min. After 80 min of disinfection, the ROS accumulated in cells was gradually consumed. Solar-driven photothermal disinfection achieved a higher inactivation efficiency in gram-positive bacteria, but the mechanism of synergy between sunlight and heat is different from *E. coli*.

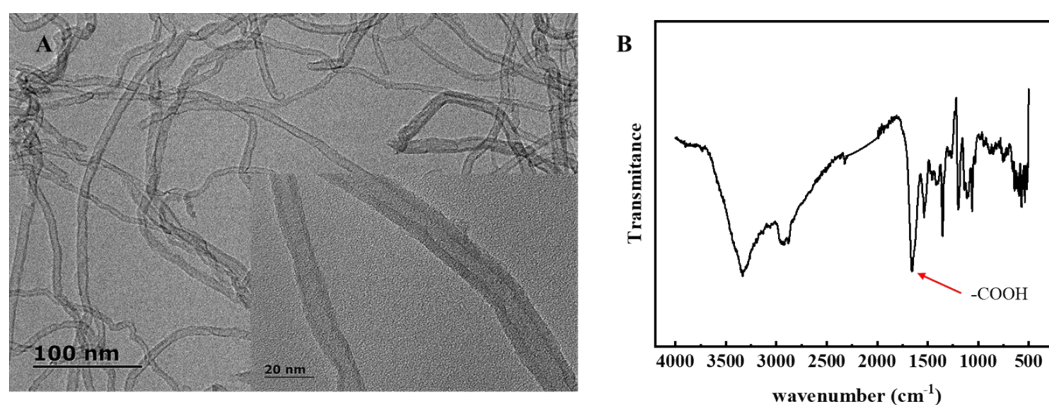


Figure S1. (A) TEM images and (B) FTIR spectra of the CNT-COOH used in the study.

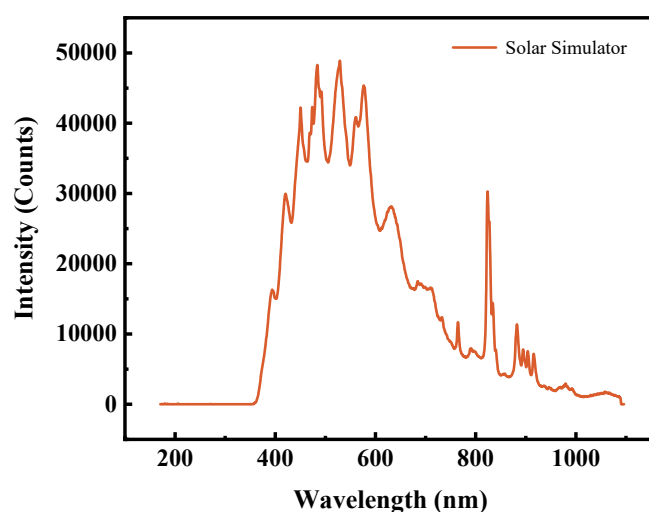


Figure S2. Wavelength of simulated solar spectrum.

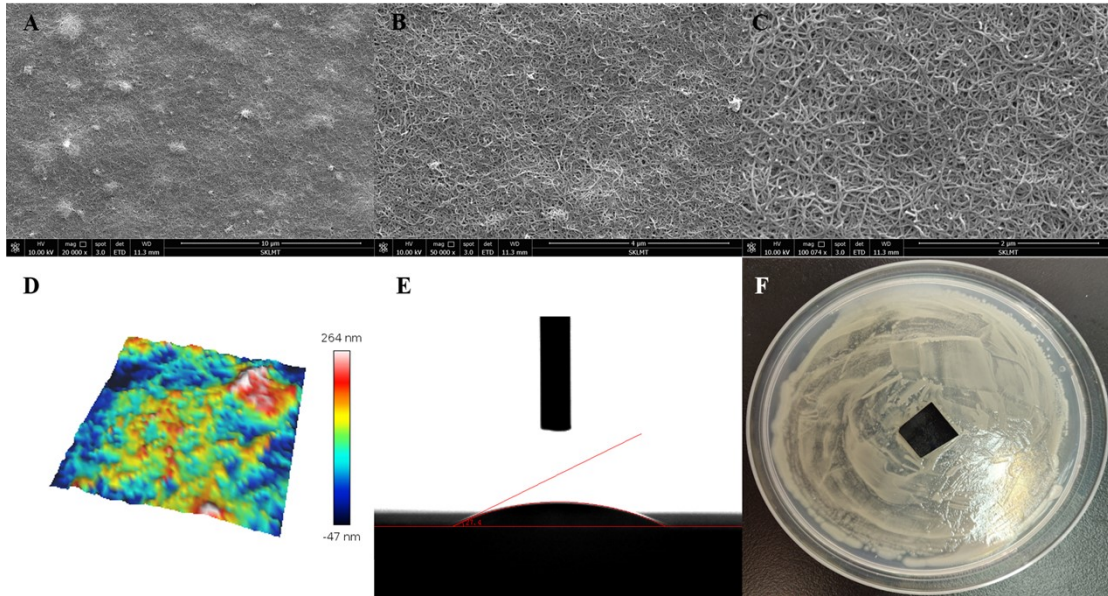


Figure S3. (A-D) Morphology of the CNT photothermal film. (A-C) SEM images (D) AFM image (scan area $4\mu\text{m}\times 4\mu\text{m}$). (E) Contact angle of the membrane. (F) Antibacterial properties of the CNT film

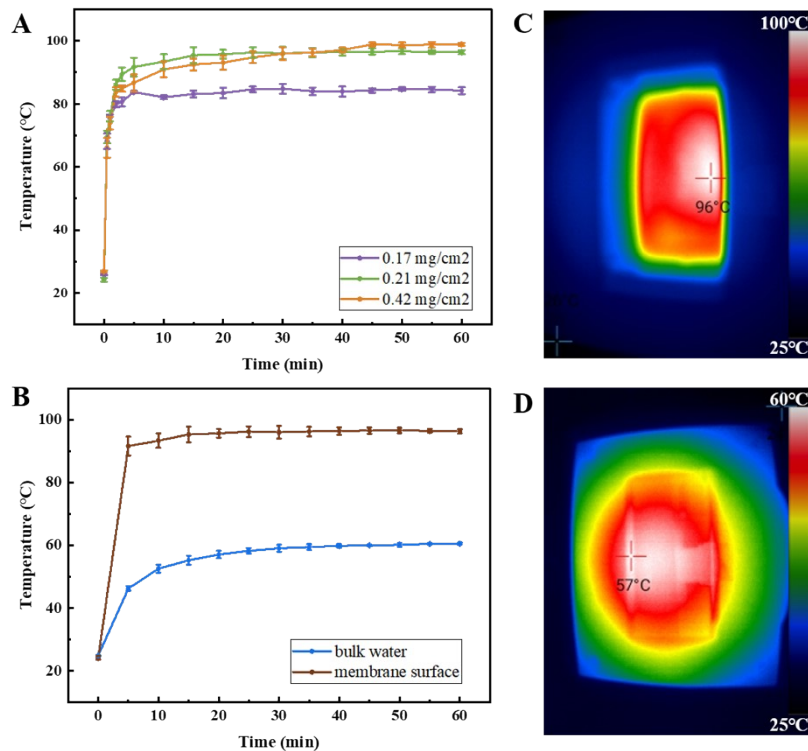


Figure S4. The photothermal heating curve of the film. (A) Surface temperature of different CNT concentration under 1 sun irradiation. (B) The film with 0.21 mg/cm^2 CNT was inserted into the reactor, then the temperature of the film surface directly irradiated by sunlight and the temperature of the water injected on the film were measured. Thermal image of (C) surface of film and (D) water on film after illumination for 20 min under 1 sun.

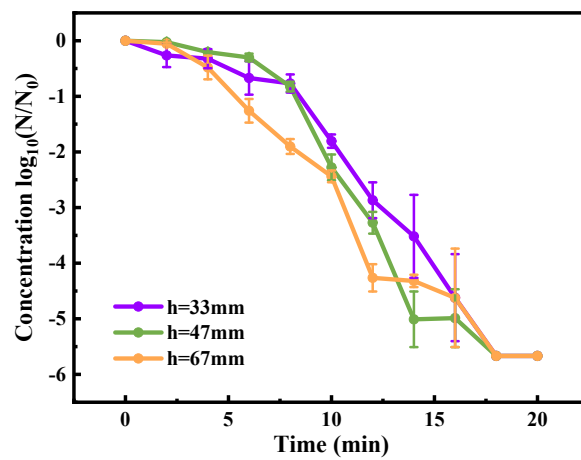


Figure S5. Inactivation of *E. coli* with different water depth (Initial bacterial concentration was $3.23\sim 4.49\times 10^5$ CFU/mL).

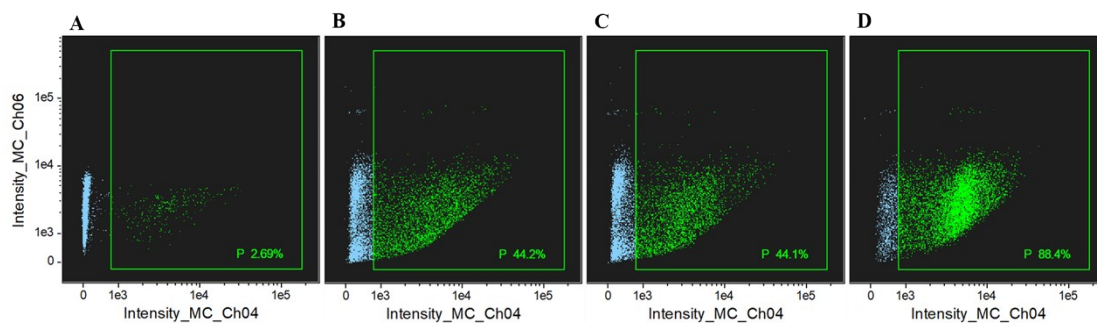


Figure S6. Levels of cell membrane destruction of *E. coli* (A) without any treatment, and subjected to (B) solar, (C) heat, and (D) photothermal disinfection. Quadrant P (PI positive) represents the percentage of damaged cell membrane.

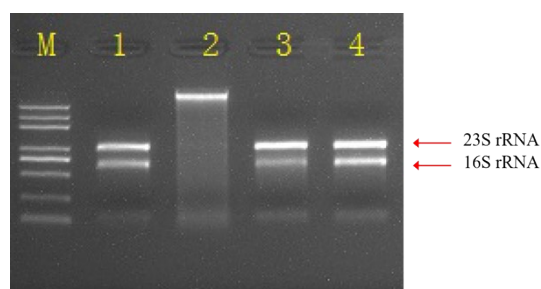


Figure S7. Extent of RNA degradation represented by agarose gel electrophoresis. 1 negative control; 2 photothermal disinfection; 3 thermal control; 4 solar control.

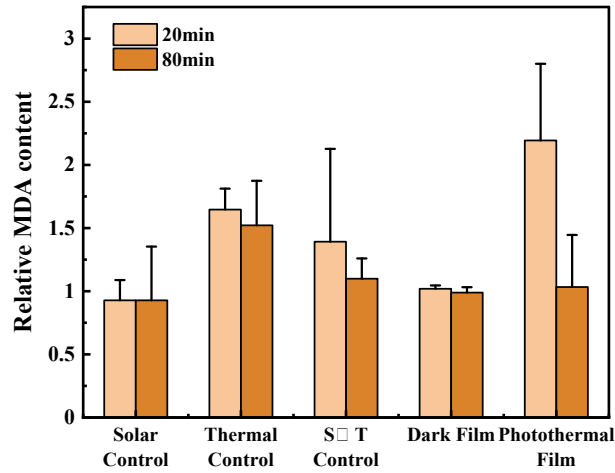


Figure S8. Relative MDA content after treatment for 20 min and 80 min. Solar control represents 1 sun solar radiation without CNT film, thermal control was incubated at 57.1 °C without solar radiation, S & T control kept in a constant temperature of 57.1 °C under 1 sun radiation without CNT film, photothermal film group is photothermal disinfection under 1 sun solar radiation and dark film group removes solar radiation on the basis of photothermal film group.

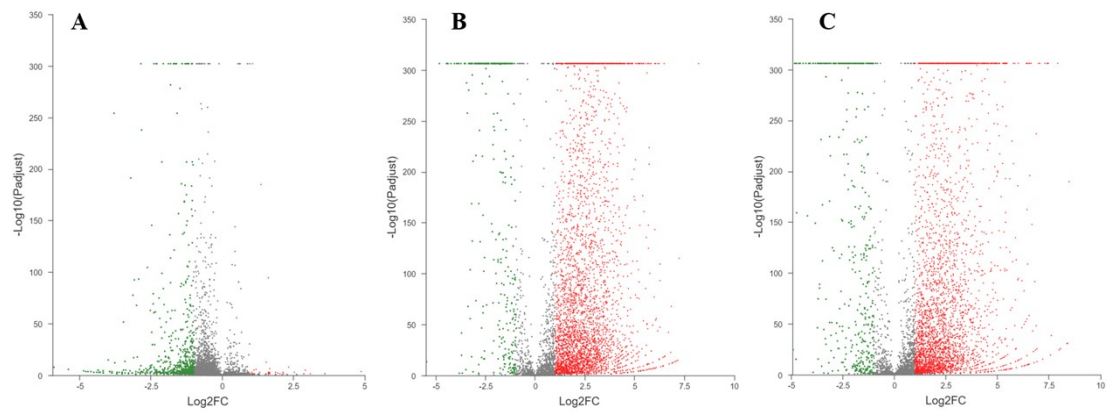


Figure S9. Volcano plot of differential gene expression in (A) solar control (B) thermal control and (C) photothermal group. The horizontal axis is the multiple change value of gene expression difference between the treated cell and original cell. The vertical axis is the P value adjusted by BH method of the difference in gene expression. The values of both horizontal and vertical coordinates are logarithmized. Each dot in the graph represents a specific gene, with red dots representing significantly upregulated genes, green dots representing significantly downregulated genes, and gray dots representing non-significantly different genes.

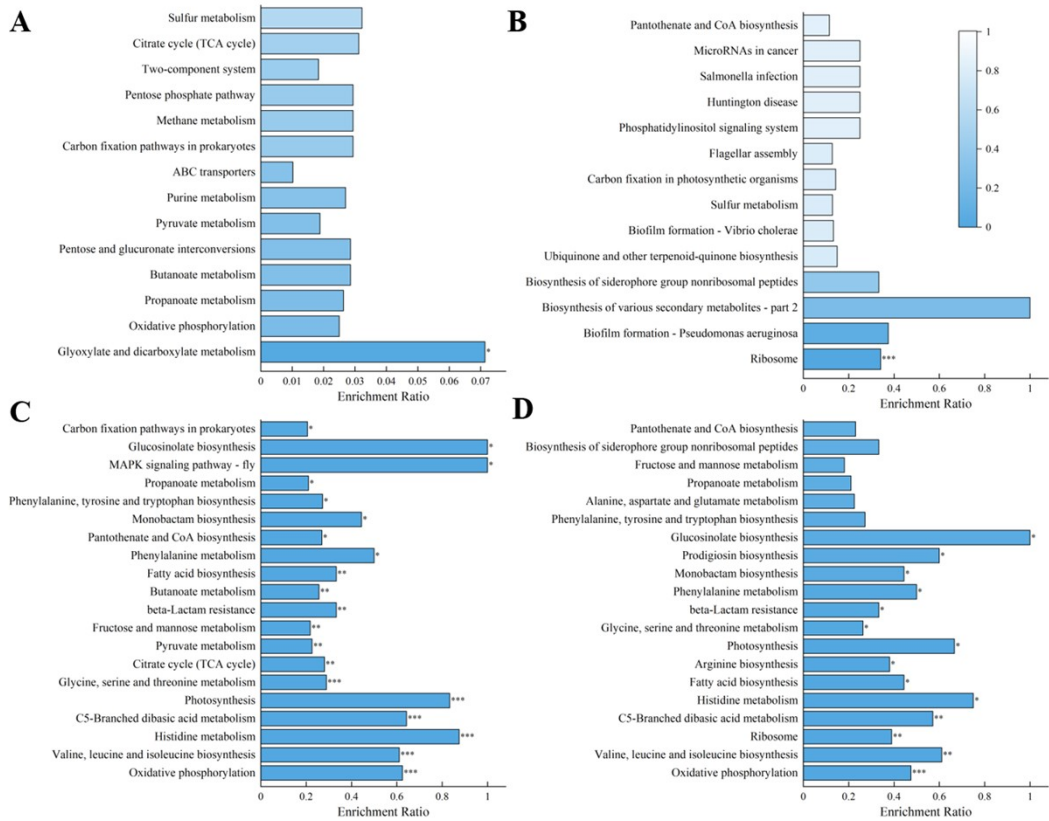


Figure S10. KEGG pathway enrichment analysis of genes (A) upregulated and (B) downregulated by solar radiation, (C) downregulated by heat stress, and (D) downregulated by photothermal disinfection. The abscissa in the figure is the pathway name, the ordinate represents enrichment rate (the ratio of the sample number of genes annotated into the pathway in the gene set to the Background number of all genes annotated into the pathway. The higher the rich factor, the greater the enrichment degree). Color represents the significance of enrichment, that is, p-adj. The darker the color, the more significant the enrichment of the pathway. P-adj<0.001 is marked as ***, p-adj <0.01 is marked as **, p-adj <0.05 is marked as *, and the color gradient on the right side represents the size of p-adj.

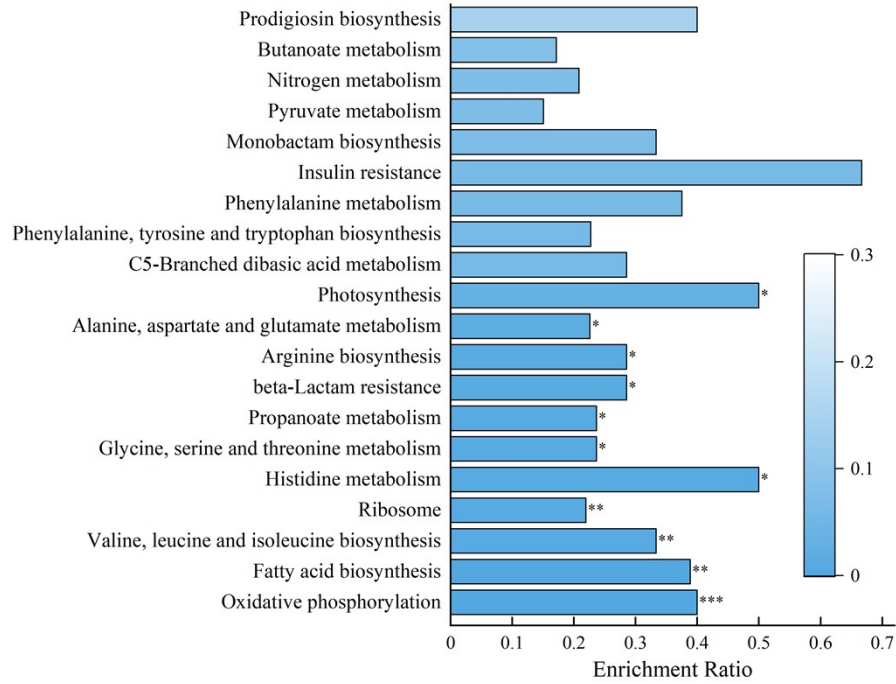


Figure S11. KEGG pathway enrichment analysis of genes downregulated in the photothermal group compared with the solar radiation group. Color represents the significance of enrichment, that is, p-adj. The darker the color, the more significant the enrichment of the pathway. P-adj<0.001 is marked as ***, p-adj <0.01 is marked as **, p-adj <0.05 is marked as *, and the color gradient on the right side represents the size of p-adj.

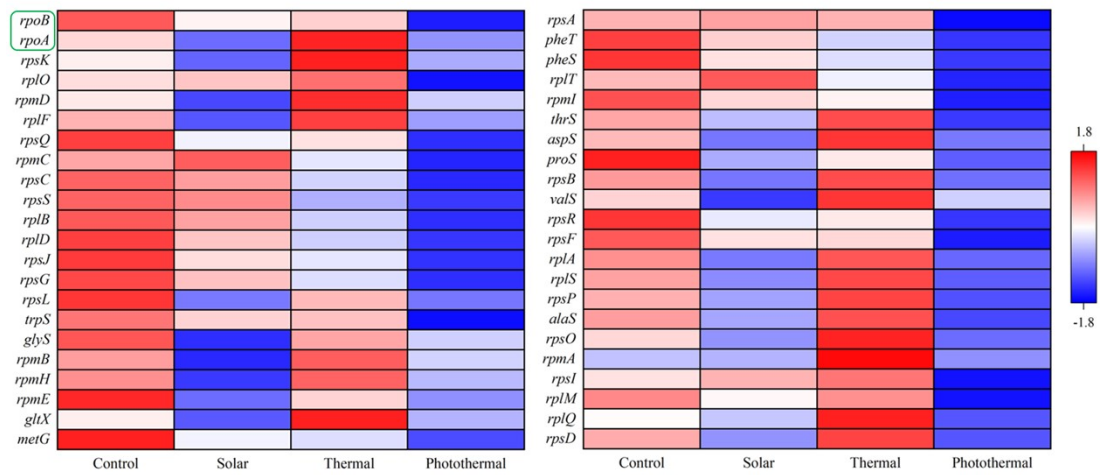


Figure S12. Gene expression heatmap related to transcription (in green circle) and translation (outside the green circle).

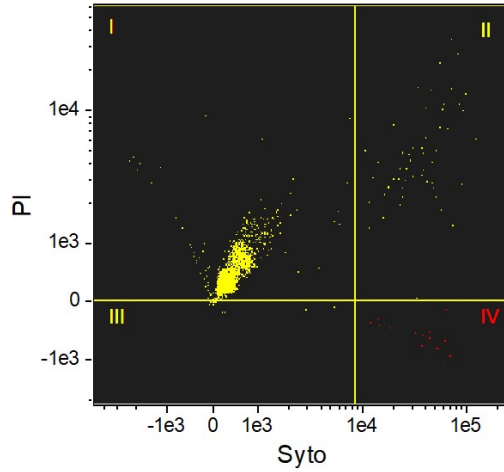


Figure S13. Living and dead cells after CNT photothermal disinfection by flow cytometry analysis. Quadrant IV (PI negative and Syto positive) represents VBNC cell.

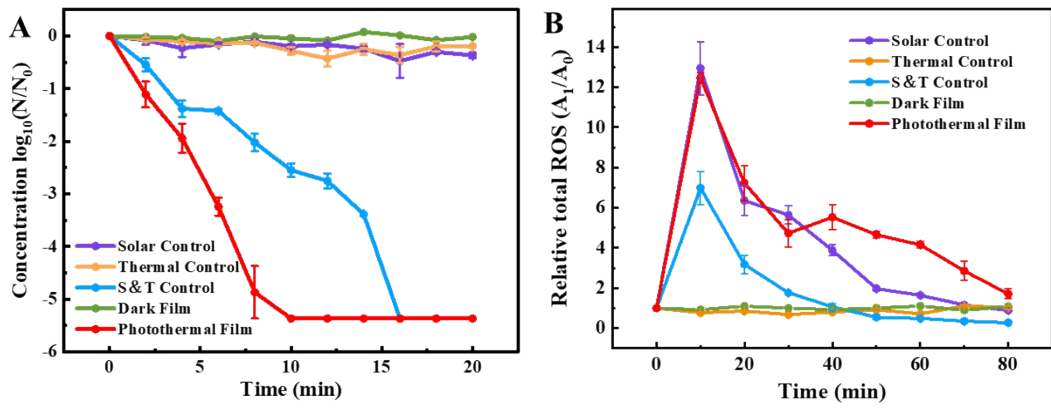


Figure S14. (A) Inactivation of *Staphylococcus aureus* under different stimulation. (B) Relative changes in the total ROS of *Staphylococcus aureus*.

Table S1. Genes related to the ribosome pathway

Gene Name	Description
<i>rpmE</i>	50S ribosomal protein L31
<i>rpmH</i>	50S ribosomal protein L34
<i>rpmB</i>	50S ribosomal protein L28
<i>rpsL</i>	30S ribosomal protein S12
<i>rpsG</i>	30S ribosomal protein S7
<i>rpsJ</i>	30S ribosomal protein S10
<i>rplD</i>	50S ribosomal protein L4
<i>rplB</i>	50S ribosomal protein L2
<i>rpsS</i>	30S ribosomal protein S19
<i>rpsC</i>	30S ribosomal protein S3
<i>rpmC</i>	50S ribosomal protein L29
<i>rpsQ</i>	30S ribosomal protein S17
<i>rplX</i>	50S ribosomal protein L24
<i>rplE</i>	50S ribosomal protein L5
<i>rpsN</i>	30S ribosomal protein S14
<i>rplF</i>	50S ribosomal protein L6
<i>rpmD</i>	50S ribosomal protein L30
<i>rplO</i>	50S ribosomal protein L15
<i>rpmJ</i>	50S ribosomal protein L36
<i>rpsM</i>	30S ribosomal protein S13
<i>rpsK</i>	30S ribosomal protein S11
<i>rpsD</i>	30S ribosomal protein S4
<i>rplQ</i>	50S ribosomal protein L17
<i>rplM</i>	50S ribosomal protein L13
<i>rpsI</i>	30S ribosomal protein S9
<i>rpmA</i>	50S ribosomal protein L27

<i>rpsO</i>	30S ribosomal protein S15
<i>rpsU</i>	30S ribosomal protein S21
<i>rpsP</i>	30S ribosomal protein S16
<i>rplS</i>	50S ribosomal protein L19
<i>rplA</i>	50S ribosomal protein L1
<i>rplJ</i>	50S ribosomal protein L10
<i>rplL</i>	50S ribosomal protein L7/L12
<i>rpsF</i>	30S ribosomal protein S6
<i>rpsR</i>	30S ribosomal protein S18
<i>rpsB</i>	30S ribosomal protein S2
<i>rpmI</i>	50S ribosomal protein L35
<i>rplT</i>	50S ribosomal protein L20
<i>rpsA</i>	30S ribosomal protein S1
DR76_RS24370	type B 50S ribosomal protein L31
<i>ykgO</i>	type B 50S ribosomal protein L36
